Chapter 8

Advancement of Sol-Gel–Prepared TiO_2 Photocatalyst

Robabeh Bashiri, Norani Muti Mohamed and Chong Fai Kait

Additional information is available at the end of the chapter

http://dx.doi.org/10.5772/intechopen.68357

Abstract

This chapter elaborates a review of sol-gel–prepared TiO_2 photocatalyst for different photocatalytic applications. Among the semiconductors employed, TiO_2 is known as an attractive photocatalyst owing to its high photosensitivity, nontoxicity, easy availability, strong oxidizing power and long-term stability. Some research works related to the effect of sol-gel preparation parameters on physicochemical properties and different photocatalytic applications of prepared TiO_2 photocatalysts are reported. Furthermore, various sol-gel and related systems for modification of TiO_2 photocatalytic performance, including transition metals and co-doing of TiO_2, were considered. The results illustrated that doping TiO_2 with metal ions through sol-gel method usually resulted in an improved efficiency of TiO_2 photocatalyst. This method has all the advantages over other preparation techniques in terms of purity, homogeneity, felicity and flexibility in introducing dopants in a large concentration, stoichiometry control, ease of processing and composition control.

Keywords: TiO_2, metal doping, hydrolysis, physicochemical properties, photocatalytic activity

1. Introduction

An excessive deal of attention has recently been paid to the development of photocatalyst which being used in a variety of products and research areas especially for environmental and energy applications. Semiconductor-based photocatalyst have been extensively studied due to its electronic configuration to absorb applied solar spectrum for photocatalytic reaction. The semiconductor consists of a valence band (VB) and conduction band (CB). The energy difference between the top of the VB and the bottom of the CB levels is known as band gap energy (Eg) which is responsible for photoactivity of the semiconductor. **Figure 1** displays the general principle of photocatalytic reaction over the semiconductor as summarized in the following steps:

1. Harvesting photons with energy equivalent or larger than the bandgap energy to form electron-hole pairs.
2. Photogenerated electrons are injected to the CB, while photogenerated holes with a positive charge are left behind in the VB.
3. Surface chemical reactions consist of reducing an acceptor species ($A^+ \rightarrow A$) and oxidizing a donor species ($D \rightarrow D^+$) [1].

Semiconducting oxides such as TiO_2, $SrTiO_3$, ZnO, α-Fe_2O_3, WO_3, Ta_2O_5, VO_2, $KTaO_3$ and Fe_2O_3 appear to be the most considered materials for photocatalysts due to the fact that their properties can be modified over wide ranges through changing their semiconducting properties. Moreover, these materials are economically promising because their processing technologies are relatively simple [2, 3]. Among different metal oxides, TiO_2 is one of the most significant photocatalyst with a large variety of applications in energy and environment (**Figure 2**),

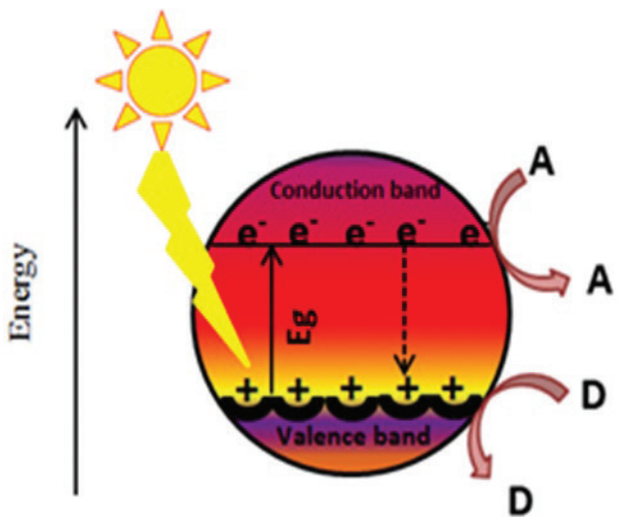

Figure 1. A schematic diagram of general principle of the photocatalytic reaction.

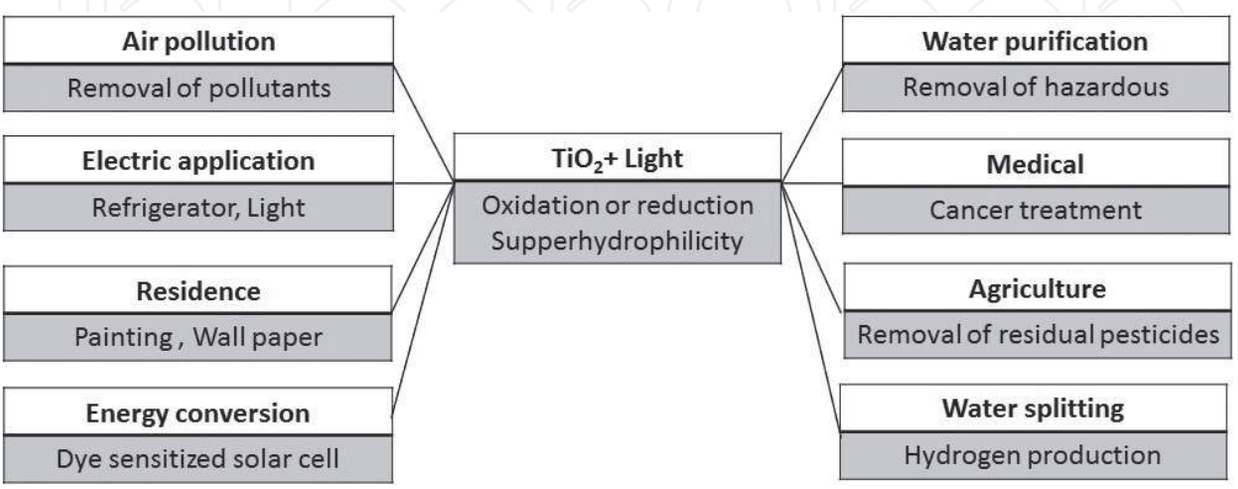

Figure 2. Different photocatalytic applications of TiO_2.

regardless of its limitations. The following section is dedicated to the discussion of the intrinsic properties of TiO_2 to fully understand its function as a photocatalyst and its synthesis process.

2. Titanium dioxide (TiO_2) photocatalyst

TiO_2 has high resistance to corrosion and photocorrosion in an aqueous medium, cheaper than many other photosensitive materials, easily available, environmentally friendly. Furthermore, its electronic properties can be varied by just changing the defect chemistry or oxygen stoichiometry [9]. The photocatalytic applications of TiO_2 are restricted because of its large bandgap energy (3.0–3.2 eV) and small electron mobility of 1 cm^2/V s [4–6]. TiO_2 has three crystalline phases, including anatase, rutile and brookite. Anatase and rutile are the most common structures for photocatalytic studies. **Figure 3a** and **b** describes the lattice structures of anatase and rutile, respectively, in the form of distorted TiO_6 octahedral with six O^{2-} ions around each Ti^{+4} ion. The structure of rutile represents an irregular octahedron with slightly orthorhombic distortion compared to octahedron in anatase [34]. The structural difference between anatase and rutile explains the significant difference in their electronic band properties.

However, rutile with band gap energy of 3.0 eV has a threshold absorption edge of 415 nm in the visible region compared to anatase with band gap energy of 3.2 eV and threshold absorption of 390 nm. Researchers have reported that anatase is the appropriate crystalline phase for photocatalytic hydrogen production [36]. It has more negative CB position (~0.2 eV) compared to rutile as demonstrated in **Figure 4**, while their VB positions (O2p) are almost in the similar position.

2.1. Sol-gel synthesis of TiO_2 nanoparticles

Photocatalytic activity of TiO_2 is strongly influenced by the synthesis condition and methodology. Various methods have been applied for synthesis of TiO_2 photocatalyst: electrochemical [7, 8], combining inverse micelle and plasma treatment [9], dip coating [10], two step wet

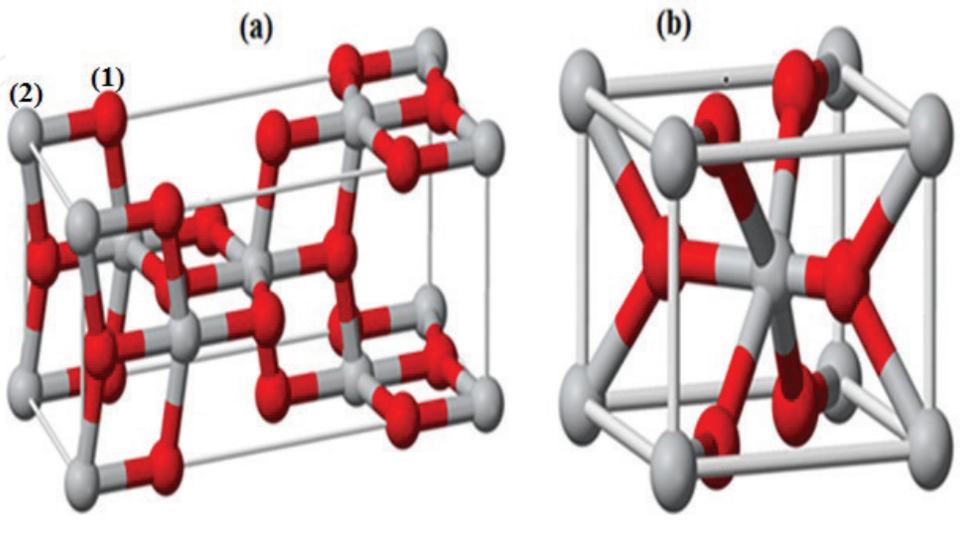

Figure 3. The bulk structural model of: (a) anatase and (b) rutile (ball (1) and (2) represent oxygen and titanium atoms, respectively) [35].

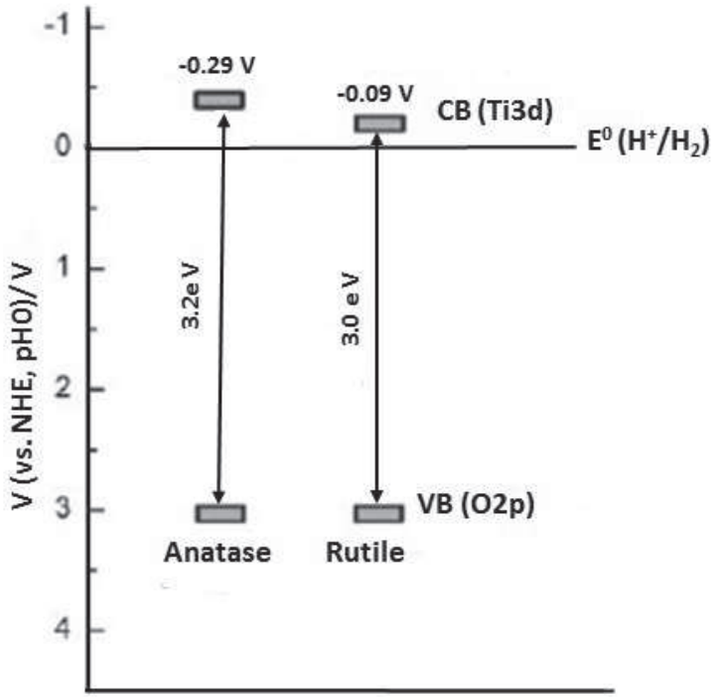

Figure 4. Electronic bands of anatase and rutile [36].

chemical [11], precipitation [12], thermal (hydrothermal and solvothermal) [13, 14], chemical solvent and chemical vapor decomposition (CSD and CVD) [15, 16], ultrasonic irradiation [17], two-route sol-gel [18], and sol-gel [19–21]. Sol-gel method is a technique to improve the physicochemical and electrochemical properties of TiO_2 nanocrystalline. It provides a simple synthesis process of nanoparticle at ambient temperature under atmospheric pressure, and this technique does not require a complicated set up. The benefits derived from preparing TiO_2 by sol-gel method (process flow chart shown in **Figure 5**) such as purity, homogeneity, and flexibility of the growth of TiO_2 can be effectively controlled by hydrolysis and condensation of titanium alkoxide in the aqueous medium [22]. Typically, sol-gel–derived precipitates are amorphous in nature, requiring further heat treatment to induce crystallization. Based on literatures, the sol-gel method has been modified using various techniques like calcination, ultrasonic [23], hydrothermal [24, 25], or surfactant [26] to obtain better properties of the synthesized powders.

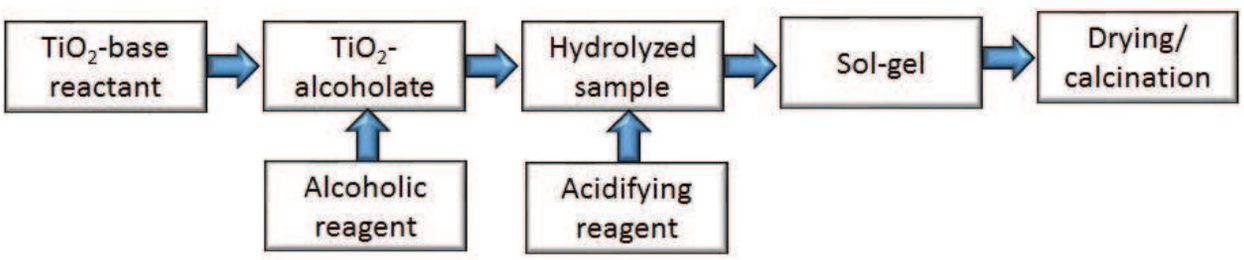

Figure 5. A schematic diagram of sol-gel process to synthesize TiO_2-based photocatalysts [22].

In normal sol-gel processing, gelation and calcintion are necessary. If the calcination temperature for crystallization is not high enough, some organic molecules will remain in the product, leading to the incomplete crystallization of titania. However, high temperature calcination causes high aggregation rate and/or phase transformation [27]. Hydrothermal synthesis provides an easy route to prepare a well-crystalline and phase-pure oxide in a tightly closed vessel. The hydrothermal-assisted sol-gel method helps to increase the number of hydroxyl groups (OH^-) on the surface of the photocatalyst and requires a lower calcination temperature. The prepared TiO_2 by this method has high thermal stability, well-crystalline phase, small particle sizes, and large surface area, which are beneficial to improve the photocatalytic activity [28–30]. The sol-gel process is typically based on the formation of inorganic polymer by hydrolysis and condensation of metal precursor like titanium alkoxide to oxopolymers, which are transformed into a metal alkoxide in aqueous solutions or organic solvents [31–34]. A number of parameters can influence on the hydrolysis process like water to alkoxide ratio, pH, and solvents. Water plays a significant role during the hydrolysis process to determine the reaction mechanism, the number of active sites on the surface of the photocatalyst and the physical properties of the photocatalyst during photocatalytic reaction [35].

2.2. Effect of hydrolysis process on sol-gel method

The water to alkoxide molar ratio (R_W) plays an important role in the structure of TiO_2 due to controlling of the formation of nucleus and the growth of crystallites. The total sol-gel synthesis can be described by an alcoholic permutation reaction, hydrolysis, and condensation reactions, which are competitive with alkoxolation, oxolation and olation as follows:

1. Alcoholic permutation

$$\mathrm{M(OR)Z} + x\,\mathrm{R'(OH)} \leftrightarrow \mathrm{M(OR)Z} - x\mathrm{(OR')} + x\mathrm{ROH} \tag{1}$$

2. Hydrolysis

$$\mathrm{M(OR)}\,n + n\mathrm{H_2O} \rightleftarrows \mathrm{M(OH)}\,n + n\mathrm{ROH} \tag{2}$$

3. Condensation reactions

A. Alcoxolation

$$\mathrm{M\text{-}OH} + \mathrm{M\text{-}OR} \rightleftarrows \mathrm{M\text{-}O\text{-}M} + \mathrm{R\text{-}OH} \tag{3}$$

B. Oxolation

$$\mathrm{M\text{-}OH} + \mathrm{M\text{-}OH} \rightleftarrows \mathrm{M\text{-}O\text{-}M} + \mathrm{H_2O} \tag{4}$$

The water to alkoxide molar ratio is investigated in two main groups: low R_W and high R_W. Hydrolysis of alkoxide with low water content less than stoichiometric ratio ($R_W < 4$) causes an incomplete hydrolysis. Therefore, unhydrolyzed alkoxide can be absorbed on the surface of TiO_2 and increase particle size with irregular shape and low surface area [36]. A high R_W ($R_W > 100$) causes the completion of nucleation and growth during the hydrolysis of TiO_2

within nanosecond; thus, TiO_2 particle is unstable, and the white suspension is immediately formed due to precipitation of a large aggregate [37]. Furthermore, adding external solvent like simple alcohols can significantly affect the controlling hydrolysis and condensation rate.

Venkatachalam et al. [38] investigated the influence of water to alkoxide ratio, pH, and type of solvent (methanol, isopropyl alcohol, acetic acid) on the physicochemical properties of TiO_2 and consequently its photocatalytic activity by using Bisphenol-A (BPA) as a model pollutant. **Table 1** illustrates that the prepared photocatalysts in the presence of acetic acid had smaller particle size and higher surface area compared to prepared TiO_2 in the presence of isopropanol and methanol. It was explained that acetic acid as a catalyst causes a rapid hydrolysis process, formation of titanium hydroxide, and their condensation to form TiO_2 nanoparticles. In addition, the variation of pH from 3 to 9 during hydrolysis process illustrates that the prepared TiO_2 photocatalyst at pH = 9 has very low surface area due to rapid hydroxylation of titanium precursor and agglomeration of TiO_2 particles.

It was reported that high water: alkoxide ratio improves the nucleophilic attack of water on titanium (IV) isopropoxide; however, it had negative effect on the surface area beyond the optimum level (350) due to more agglomeration. Furthermore, the presence of residual alkoxy groups decreases the crystallization rate of TiO_2, which favor the formation of less dense anatase phase exclusively. At low water content, the hydrolysis rate is slow, and the existence of excess titanium alkoxide in the solvent favors the development of Ti–O–Ti chains and formation of high ratio of rutile phase. They reported that the synthesized TiO_2 photocatalyst under the optimum molar ratio of alkoxide, acetic acid and water is 1:10:350 had maximum photocatalytic mineralization of BPA over nano-sized TiO_2 photocatalystcompered to P25 (commercial TiO_2) and other prepared photocatalysts.

Bashiri et al. [29] reported synthesis a series of 10 mol% Cu/TiO_2 photocatalysts by varying H_2O:alkoxide molar ratios (8, 16, 32, and 64) using sol-gel–associated hydrothermal method. The influence of hydrolysis rate on the physicochemical properties (**Table 2**) and photocatalytic

Photocatalyst	BET surface area (m^2 g^{-1})	Catalyst anatase crystallite size (nm)	Anatase:rutile ratio (%)	Band gap energy (eV)
Hydrolyzing agent				
Methanol	69	17	69:31	3.19
Isopropyl alcohol	84	12.6	74.26	3.21
Glacial acetic acid	107	8.3	82.18	3.27
Source:solvent:water				
1:10:150	86	12	73:27	3.19
1:10:250	94	10.1	78:22	3.26
1:10:350	110	8.1	83:17	3.28
1:10:450	91	8.6	74:26	3.21

Table 1. Physicochemical properties of nano-sized TiO_2 photocatalysts [38].

Photocatalysts	H_2O:alk xide	Crystallite size (nm)	Average particle size (nm)		BET surface area (m^2/g)	Band gap (eV)	Hydrogen production (μmol)
			TEM	FESEM			
TiO_2	0	13.55	13.89	27.54	82.69	3	24.5
CuT8	8	9.63	11.47	22.194	85.57	2.96	1228.8
CuT16	16	11.22	12.08	19.72	83.5	2.9	3926.8
CuT32	32	12.88	13.34	16.835	89.19	2.72	10571.0
CuT64	64	10.54	12.53	20.185	84.57	2.83	3010.3

Table 2. Physicochemical properties of all prepared photocatalysts [29].

hydrogen production by water photosplitting in an aqueous NaOH-glycerol solution were investigated. It was demonstrated that the amount of water has strong influence on the hydrolysis and polymerization rate, changing the physicochemical properties and photocatalytic activity of the prepared photocatalysts.

The average crystal sizes ranged from 9.63 (CuT8) to 13.55 nm (TiO_2), which confirmed that the presence of copper and variation of water contents can strongly control crystal size. The low water content (CuT8) causes the incomplete hydrolysis, leads to aggregates, and surpasses the crystal growth. However, adding more water showed negative impact on the crystallinity due to formation of aggregates rather than the growth of crystals, strong nucleophilic reaction and fast hydrolysis rate. In this case, more alkoxy groups in the alkoxide are substituted by hydroxyl groups from H_2O, and the quantity of unhydrolyzed alkyl in the precursor is reduced hence reduction in steric hindrance by the residual alkyls preventing crystallization to anatase phase [37, 39]. The better crystallinity and proper crystal size of CuT32 compared to other photocatalysts can be explained by the moderate hydrolysis rate during preparation. The variation of the BET surface area of mesoporous photocatalysts from 82.69 to 89.19 m^2/g illustrates that the grain size was decreased in CuT8 and CuT64 but the surface area did not increase due to the agglomeration during hydrolysis process. The photocatalyst with the H_2O:alkoxide molar ratio of 32 produced the highest cumulative hydrogen production of 10571 μmol in 300 min compared to TiO_2 and other synthesized Cu/TiO_2 photocatalysts in the aqueous NaOH-glycerol solution. The mesoporous nanoparticles with larger specific surface area, lower bandgap energy, more absorbance in the visible region, presence of Ti^{3+} with higher photocatalytic activity and the coexistence of Cu_2O and CuO are responsible for better photocatalytic performance of CuT32 photocatalyst.

In the other work, Behnajady et al. [40] synthesized titanium dioxide nanoparticles by sol-gel method. Various precursors under different synthesis conditions such as solvent and water percent, reflux temperature and time, sol drying method and calcination temperature are studied as shown in **Table 3**.

The photocatalytic activity of prepared TiO_2 was studied by photodegradation of C.I. Acid Red 27 as a model contaminant from textile industry under UV light irradiation. Results of characterization revealed that the type of the precursor and solvent is effective on the particle size

Parameter	Variations
Precursor	Titanium tetraisopropoxide (TTIP), titanium n-butoxide (TBOT)
Solvent	Methanol, ethanol, isopropanol
Solvent molar percent (%)	1, 5, 10, 15, 20
Water molar percent (%)	10, 20, 40, 65, 80, 100
Reflux temperature (°C)	50, 65, 80
Reflux time (h)	1, 3, 6
Sol drying method	Thermal drying, freeze drying
Calcination temperature (°C)	350, 450, 750

Table 3. Experimental parameters [40].

and crystalline structure of the synthesized TiO_2 nanoparticles, which can strongly control the photocatalytic performance of TiO_2. Optimal conditions for synthesis of TiO_2 nanoparticles with excellent photocatalytic activity were obtained from titanium isopropoxide precursor in methanol solvent with molar ratio of 1:65:1(precursor:water:solvent) under reflux for 3 h at reflux temperature of 80°C, employing thermal drying method for sol drying and calcination temperature of 450°C. Titanium dioxide nanoparticles produced under optimal conditions show higher photocatalytic activity than commercial TiO_2-P25. In the following section, the various sol-gel and related systems of doping TiO_2 including noble metal, co-doping, transition metal doping, and their photocatalytic performance in degradation of pollutants in aqueous solutions and solar hydrogen production are discussed.

3. Doped-TiO_2 photocatalysts by sol-gel method

Many researchers have attempted to modify TiO_2 surface to overcome its limitation for photocatalytic reaction. The aim of these modifications is to extend the absorbance edge into the visible region, reducing charge carrier recombination and decreasing fast backward reaction. The modification of TiO_2 mainly was conducted through the following strategies:

1. Doping metal ions with a $\mathbf{d^n}$ ($0 < n < 10$) electronic configuration
2. Valence band control using an anion's **p** orbitals or the **s** orbital of p-block metal ions
3. Spectral sensitization [41]

The metal dopant can strongly influence on the number of surface defects by changing the morphology such as crystal structure, crystallinity and particle size [1, 42]. Type of metal dopants (electronegativity and affinity), total metal loading, preparation method, and chemical state of metal are crucial parameters to control the effect of metal loading in TiO_2 [28]. In this

section, we discuss various sol-gel and sol-gel–related systems of doping TiO_2, including co-doping, transition metal and their photocatalytic performance.

3.1. Noble metal–doped TiO_2 by sol-gel method

Loading noble metals (platinum (Pt), rhodium (Rh), palladium (Pd), silver (Ag) and gold (Au) with a low overpotential have been investigated as the effective materials to enhance photocatalytic activity in terms of hydrogen production on the surface of TiO_2 [48–56]. **Figure 6** displays that their Fermi energy levels are lower than TiO_2 and the formation of Schottky barrier helps (retarding the electron/hole recombination) to pass photo-excited electrons from the CB of TiO_2 to the deposited metal particles on the surface of TiO_2 until achieving a thermodynamic equilibrium and their Fermi level energy are aligned [43]. Hence, accumulation of electrons in the noble metal particles is caused that their Fermi levels shift to more negative and closer to the CB level of TiO_2, which is suitable for the reduction of water to hydrogen. Pt and Au have been used intensively as a co-catalyst compared with other noble metals due to their lower overpotential, desirable electron affinity and work function compared to other noble metals [44].

Rosseler et al. described a comparison between sol-gel–prepared Au and Pt-doped TiO_2. They showed that the optimum photocatalyst of 3 wt%-Au/TiO_2 produced maximum amount of hydrogen up to 120 μmol/min in methanol (1, v/v%) solution under 150 W metal halide lamp (large portion of the visible light range) with intensity of 30 mW/cm^2. Low photocatalytic activity of Pt/TiO_2 was corresponded to low extension of absorption edge to the visible and great activity of Pt toward backward reaction:(H_2 + 1/2 $O_2 \rightarrow H_2O$) even at room temperature. Furthermore, they pointed out that the photocatalytic activity of a photocatalyst can be tuned by following considerable parameters:

1. The type and content of the metallic co-catalyst and metal-support interactions
2. The surface crystallographic, anatase/rutile ratio, porosity properties of the TiO_2
3. The relative amount of methanol added as sacrificial agent [38]

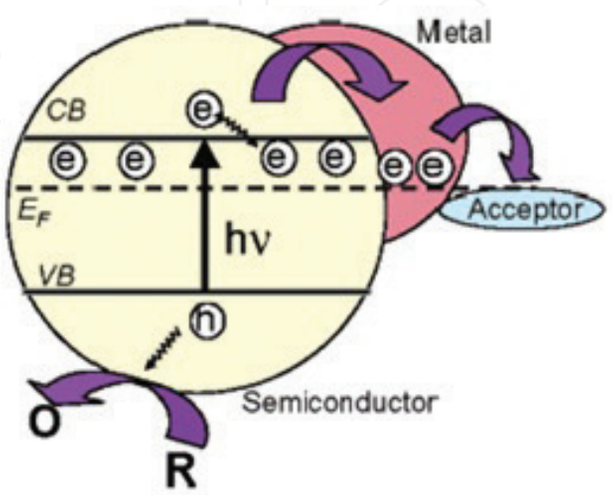

Figure 6. Fermi level equilibration in a semiconductor-metal nanocomposite [43].

Naseri et al. [45] synthesized sol-gel-derived Ag/TiO_2 thin films with various Ag:Ti molar ratios of 0, 1, 2, 5, 10 and 20 mol%. Ag/TiO_2 photocatalyst was immersed in 1 M KOH as the photoanode, Pt wire as the cathode, and Ag/AgCl as the reference electrode (RE) under the illumination of Xe short arc lamp with intensity of 1000 W/m^2 to measure photoelectrochemical activity. The 1 mol% Ag doped TiO_2 photocatalyst (crystallite size: 11 nm) had maximum photocurrent density of 0.8 mA/cm^2 and hydrogen production rate of 197 μmol/h. The modification of TiO_2 with noble metals is the promising method, but their high cost and relatively low availability strongly limit their application for large-scale photocatalytic systems. Therefore, largely available and cheap transition metals with acceptable photocatalytic activity can replace with the noble metals [46–49].

3.2. Transition metal–doped TiO_2 by sol-gel method

Transition metal (Cr, Mn, Fe, Co, Ni, Cu, and Zn) doped TiO_2 nanoparticles were synthesized by the sol-gel method using 2-hydroxylethylammonium format as an ionic liquid by Ghasemi et al. [50]. The performance of prepared photocatalysts was evaluated by degradation of Acid Blue92 (AB92) in aqueous medium under UV light. The results illustrated that transition metal (TM) doped TiO_2 nanoparticles was significantly enhanced photodegradation of AB92 in water compared to pure TiO_2. The studies revealed that transition metal (TM) doped TiO_2 nanoparticles have smaller crystalline size and higher surface area than pure TiO_2. Dopant ions in the TiO_2 structure caused significant absorption shift into the visible region. They explained that this better photocatalytic degradation may correspond to high electron-hole generation and low charge carrier recombination rate. The Fe/TiO_2 photocatalyst displayed maximum efficiency rate constant for AB92 degradation. The reason for the highest activity of Fe/TiO_2 could be the lowest crystalline size, the highest surface area and the minimum band gap energy. A decrease in crystallite size can give rise to larger surface area, which can increase the available surface active site and consequently leads to a higher adsorption of dye, separationof electron-hole generation, and interfacial charge carrier transfer rate for degradation. The photocatalytic hydrogen production of prepared NiO/TiO_2 photocatalysts with sol-gel and conventional incipient wetness impregnation methods was investigated by Sreethawong et al. [51]. They observed that sol-gel–prepared NiO/TiO_2 under 300 W high-pressure Hg lamp in an aqueous methanol solution had markedly higher hydrogen production rate of 162.6 μmol/h compared to TiO_2 photocatalyst (87.2 μmol/h). Furthermore, they pointed out that the extending absorption edge of NiO/TiO_2 to the longer wavelengths between 600 to 800 nm and combination of single-step sol-gel process with pore-controlling surfactant caused high photocatalytic performance. Singh et al. [52] studied the photoelectrochemical performance of synthesized anatase Fe/TiO_2 photoanode with sol-gel spin coating method. The photoelectrochemical behavior of Fe/TiO_2 photoanode was explored under 150 W Xenon Arc lamp and reaction condition; electrolyte: NaOH with pH = 13, cathode: Pt and reference electrode (RE): saturated calomel electrode (SCE). The four layers of 0.2 at % Fe/TiO_2 photoanode with thickness of 1.30 μm showed better shift of the absorption edge toward the visible region with bandgap energy of 2.89 eV. In addition, the measured photocurrent density (jp was ~0.92 mA/cm^2 at zero external bias. Many researchers have been reported that co-doped TiO_2 is more effective technique to

improve the photocatalytic performance of TiO_2 compared to single-doped TiO_2 due to the synergistic effect of the presence of two metals.

3.3. Co-doped TiO_2 by sol-gel method

The photocatalytic properties of bimetallic nanoparticles are directly related to their composition structure and catalyst preparation processes. Kim et al. [53] synthesized Cu-Ag/TiO_2 photocatalyst with the sol-hydrothermal method (to split water under UV irradiation with intensity of 18 W/cm^2 in the presence of methanol. The $Cu_{(0.03)}$-Ag $_{(0.07)}$ $Ti_{(0.9)}O_2$ photocatalyst (crystallite size: 15.28 nm) markedly increased hydrogen production rate up to 1093 mmol/h compared to Ag/TiO_2 (312 mmol/h), Cu/TiO_2 (900 mmol/h), and TiO_2 (200 mmol/h). They suggested that the Cu or Ag components in the TiO_2 framework were reduced by attracting the excited electrons from the valence band of TiO_2, because of the greater reduction potential of CuO or AgO than that of pureTiO_2. This hinders the recombination of charge carriers because the CuO or AgO component captures electrons, thereby increasing the number of holes over the valence band and allowing methanol decomposition to continue. Sun et al. [28] synthesized the single (Fe and Ni) and bimetallic (Fe-Ni) doped TiO_2 using the sol-hydrothermal method. They found out that 5% Fe-4% Ni/TiO_2 photocatalyst (crystallite size:13.8 nm, surface area: 98.35 m^2/g, and bandgap energy: 2.41 eV) had the maximum hydrogen production rate of 361.64 μmol/h.gcat compared to other metal loading ratios under a 500 W Xenon lamp equipped with a 400 nm cut-off glass filter in an aqueous ethanol solution. This result was corresponded to better ability of charge carrier separation, restriction of their recombination and red shifting absorption edge to 514 nm compared to TiO_2. In the other works, Sun et al. [54] successfully synthesized Ag and Fe doped TiO_2 using sol-hydrothermal method. The water photosplitting was conducted in an aqueous ethanol solution with two light sources: A 16-W high-pressure inner irradiation Hg lamp (λ = 254 nm) with intensity of 11.7 mW/cm^2 as the UV light source and 500 W Xe lamp equipped with a 400 nm cut-off glass as the visible light source. 4.5% Fe-4.5% Ag/TiO_2 photocatalyst (crystallite size: 12.1 nm, bandgap energy: 2.03 eV, and particle size: 12 nm) had a higher hydrogen production rate of 515.45 μmol/h.gcal compared to monometallic doped and undoped TiO_2. They concluded that the interaction of Fe and Ag with TiO_2 reduces particle size (~12 nm), shifts absorption edge into the visible region compared to anatase phase of TiO_2 ($\lambda \leq$ 367 nm), reduces charge carrier recombination, and enhances the photocatalytic performance. **Tables 3** and **4** show a summary of reported related work to modify TiO_2 with metal dopants.

Cocatalyst	Finding	Ref	Year
Ni	The extending absorption edge of NiO/TiO_2 to the long wavelengths between 600 and 800 nm and combination of single-step sol-gel process with pore-controlling surfactant caused high photocatalytic performance	[51]	2005
Fe	0.2 at.% Fe/TiO_2 had the lowest bandgap energy of 2.89 eV, maximum jp ~0.92 mA/cm^2 at zero external bias, donor density (N_D):4.3 × 1019 cm^{-3} and more negative flat band potential (Vfb): −0.92 compared with TiO_2	[52]	2008
Cr, Mn, Fe, Co, Ni, Cu, and Zn	The most active photocatalyst was Fe/TiO_2 with maximum photocatalytic degradation rate for AB92 degradation. The reason for the highest activity could be the lowest crystalline size, the highest surface area and the minimum band gap energy	[50]	2009

Cocatalyst	Finding	Ref	Year
Ag	1 mol% Ag/TiO_2 compared with other ratios: 0, 1, 2, 5, 10 and 20 mol% had the maximum hydrogen production rate of 196 μmol/h, N_D: 16.3 × 10^{21} cm^{-3}, V_{fb}: −1.14 V and jp ~8 mA/cm^2.	[45]	2012
Cu-Ag	The Cu-Ag/TiO_2 improved the H_2 production rate up to1093 mmol/h	[53]	2012
Fe-Ni	4wt% Fe–5%Ni/TiO_2 with low bandgap energy and more red shifting of absorption edge had a high hydrogen production rate of 361.64 μmol/h	[28]	2012
Ag-Fe	The higher photocatalytic hydrogen production with the rate of 515.45 μmol/h. gcat was belong to 4.5%Ag–4.5% Fe/TiO_2 compared to hydrogen production rate single metal doped and undoped TiO_2	[54]	2013

Table 4. Summary of transition metal–doped TiO_2 (single and co-doped).

4. Conclusion

Here, the previous research works confirm that sol-gel process is a simple and easy means of synthesizing nanoparticles at ambient temperature under atmospheric pressure, and this technique does not require complicated setup. The results of the investigation conclude that optimization of preparation conditions is essential for obtaining nanocrystalline TiO_2 materials with notably higher activity than Degussa (P-25) TiO_2. Doping TiO_2 with metals is favorable to improve the photocatalytic efficiency of the catalyst in sol-gel method compared to other methods. Furthermore, from the results available, it can be concluded that co-doping of TiO_2 generally enhances the photocatalytic efficiency of the catalyst compared to single doped TiO_2.

Acknowledgements

The authors would like to thank Centre of innovative Nanostructures & Nanodevices (COINN) and Universiti Teknologi PETRONAS for financial and technical support in making this research work feasible.

Author details

Robabeh Bashiri[1]*, Norani Muti Mohamed[1,2] and Chong Fai Kait[2]

*Address all correspondence to: susanbashiri@gmail.com

1 Centre of Innovative Nanostructures & Nanodevices (COINN), Universiti Teknologi PETRONAS, Bandar Seri Iskandar, Perak, Malaysia

2 Fundamental and Applied Sciences Department, Universiti Teknologi Petronas, Bandar Seri Iskandar, Perak, Malaysia

References

[1] Kudo A, Miseki Y. Heterogeneous photocatalyst materials for water splitting. Chemical Society Reviews. 2009;**38**(1):253–278

[2] Zhu J, Zäch M. Nanostructured materials for photocatalytic hydrogen production. Current Opinion in Colloid & Interface Science. 2009;**14**(4):260–269. doi:10.1016/j.cocis.2009.05.003

[3] Bak T, Nowotny J, Rekas M, Sorrell CC. Photo-electrochemical hydrogen generation from water using solar energy. Materials-related aspects. International Journal of Hydrogen Energy. 2002;**27**(10):991–1022. doi:10.1016/s0360-3199(02)00022-8

[4] Dholam R, Patel N, Adami M, Miotello A. Physically and chemically synthesized TiO_2 composite thin films for hydrogen production by photocatalytic water splitting. International Journal of Hydrogen Energy. 2008;**33**(23):6896–6903. doi:10.1016/j.ijhydene.2008.08.061

[5] Yu J, Wang B. Effect of calcination temperature on morphology and photoelectrochemical properties of anodized titanium dioxide nanotube arrays. Applied Catalysis B: Environmental. 2010;**94**(3–4):295–302. doi:10.1016/j.apcatb.2009.12.003

[6] Hendry E, Wang F, Shan J, Heinz TF, Bonn M. Electron transport in TiO_2 probed by THz time-domain spectroscopy. Physical Review B. 2004;**69**(8):081101

[7] Karuppuchamy S, Suzuki N, Ito S, Endo T. A novel one-step electrochemical method to obtain crystalline titanium dioxide films at low temperature. Current Applied Physics. 2009;**9**(1):243–248. doi:10.1016/j.cap.2008.02.004

[8] Fan L, Ichikuni N, Shimazu S, Uematsu T. Preparation of Au/TiO_2 catalysts by suspension spray reaction method and their catalytic property for CO oxidation. Applied Catalysis A: General. 2003;**246**(1):87–95. doi:10.1016/S0926-860X(03)00002-4

[9] Arimitsu N, Nakajima A, Kameshima Y, Shibayama Y, Ohsaki H, Okada K. Preparation of cobalt–titanium dioxide nanocomposite films by combining inverse micelle method and plasma treatment. Materials Letters. 2007;**61**(11–12):2173–2177. doi:10.1016/j.matlet.2006.08.044

[10] Kluson P, Luskova H, Cajthaml T, Solcova O. Non-thermal preparation of photoactive titanium (IV) oxide thin layers. Thin Solid Films. 2006;**495**(1–2):18–23. doi:10.1016/j.tsf.2005.08.275

[11] Gu D-E, Yang B-C, Hu Y-D. V and N co-doped nanocrystal anatase TiO_2 photocatalysts with enhanced photocatalytic activity under visible light irradiation. Catalysis Communications. 2008;**9**(6):1472–1476. doi:10.1016/j.catcom.2007.12.014

[12] Dvoranová D, Brezová V, Mazúr M, Malati MA. Investigations of metal-doped titanium dioxide photocatalysts. Applied Catalysis B: Environmental. 2002;**37**(2):91–105. doi:10.1016/S0926-3373(01)00335-6

[13] Feng X, Wang Q, Wang G, Qiu F. Preparation of nano-TiO_2 by ethanol-thermal method and its catalytic performance for synthesis of dibutyl carbonate by transesterification. Chinese Journal of Catalysis. 2006;**27**(3):195–196. doi:10.1016/S1872-2067(06)60011-9

[14] Zhu J, Deng Z, Chen F, Zhang J, Chen H, Anpo M, Huang J, Zhang L. Hydrothermal doping method for preparation of Cr^{3+}-TiO_2 photocatalysts with concentration gradient distribution of Cr^{3+}. Applied Catalysis B: Environmental. 2006;**62**(3–4):329–335. doi:10.1016/j.apcatb.2005.08.013

[15] Babelon P, Dequiedt AS, Mostéfa-Sba H, Bourgeois S, Sibillot P, Sacilotti M. SEM and XPS studies of titanium dioxide thin films grown by MOCVD. Thin Solid Films. 1998;**322**(1–2):63–67. doi:10.1016/S0040-6090(97)00958-9

[16] Kim B-H, Lee J-Y, Choa Y-H, Higuchi M, Mizutani N. Preparation of TiO_2 thin film by liquid sprayed mist CVD method. Materials Science and Engineering: B. 2004;**107**(3):289–294. doi:10.1016/j.mseb.2003.12.010

[17] Peng F, Cai L, Yu H, Wang H, Yang J. Synthesis and characterization of substitutional and interstitial nitrogen-doped titanium dioxides with visible light photocatalytic activity. Journal of Solid State Chemistry. 2008;**181**(1):130–136. doi:10.1016/j.jssc.2007.11.012

[18] Huang M, Xu C, Wu Z, Huang Y, Lin J, Wu J. Photocatalytic discolorization of methyl orange solution by Pt modified TiO_2 loaded on natural zeolite. Dyes and Pigments. 2008;**77**(2):327–334. doi:10.1016/j.dyepig.2007.01.026

[19] Liao DL, Badour CA, Liao BQ. Preparation of nanosized TiO_2/ZnO composite catalyst and its photocatalytic activity for degradation of methyl orange. Journal of Photochemistry and Photobiology A: Chemistry. 2008;**194**(1):11–19. doi:10.1016/j.jphotochem.2007.07.008

[20] Zhang X, Liu Q. Preparation and characterization of titania photocatalyst co-doped with boron, nickel, and cerium. Materials Letters. 2008;**62**(17–18):2589–2592. doi:10.1016/j.matlet.2007.12.061

[21] Crişan M, Brăileanu M, Răileanu M, Zaharescu M, Crişan D, Drăgan N, Anastasescu M, Ianculescu A, Niţoi I, Marinescu VE, Hodorogea SM. Sol–gel S-doped TiO_2 materials for environmental protection. Journal of Non-Crystalline Solids. 2008;**354**(2–9):705–711. doi:10.1016/j.jnoncrysol.2007.07.083

[22] Akpan UG, Hameed BH. The advancements in sol–gel method of doped-TiO_2 photocatalysts. Applied Catalysis A: General. 2010;**375**(1):1–11. doi:10.1016/j.apcata.2009.12.023

[23] Wei X, Wang H, Zhu G, Chen J, Zhu L. Iron-doped TiO_2 nanotubes with high photocatalytic activity under visible light synthesized by an ultrasonic-assisted sol-hydrothermal method. Ceramics International. 2013;**39**(4):4009–4016. doi:10.1016/j.ceramint.2012.10.251

[24] Huang C-H, Yang Y-T, Doong R-A. Microwave-assisted hydrothermal synthesis of mesoporous anatase TiO_2 via sol–gel process for dye-sensitized solar cells. Microporous and Mesoporous Materials. 2011;**142**(2–3):473–480. doi:10.1016/j.micromeso.2010.12.038

[25] Norani MM, Bashiri R, Chong FK, Sufian S, Kakooei S. Photoelectrochemical behavior of bimetallic Cu–Ni and monometallic Cu, Ni doped TiO_2 for hydrogen production. International Journal of Hydrogen Energy. 2015;**40**(40):14031–14038. doi:10.1016/j.ijhydene.2015.07.064

[26] Liu GQ, Jin ZG, Liu XX, Wang T, Liu ZF. Anatase TiO_2 porous thin films prepared by sol-gel method using CTAB surfactant. Journal of Sol-Gel Science and Technology. 2007;**41**(1):49–55. doi:10.1007/s10971-006-0122-9

[27] Chen-Chi Wang JYY. Sol-gel synthesis and hydrothermal processing of anatase and rutile titania nanocrystals. Chemistry of Materials. 1999;**11**:3113–3120

[28] Sun T, Fan J, Liu E, Liu L, Wang Y, Dai H, Yang Y, Hou W, Hu X, Jiang Z. Fe and Ni co-doped TiO_2 nanoparticles prepared by alcohol-thermal method: Application in hydrogen evolution by water splitting under visible light irradiation. Powder Technology. 2012;**228**:210–218. doi:10.1016/j.powtec.2012.05.018

[29] Bashiri R, Mohamed NM, Kait CF, Sufian S. Hydrogen production from water photosplitting using Cu/TiO_2 nanoparticles: Effect of hydrolysis rate and reaction medium. International Journal of Hydrogen Energy. 2015;**4**(18):6021–6037. doi:10.1016/j.ijhydene.2015.03.019

[30] Bashiri R, Mohamed NM, Fai Kait C, Sufian S. Influence of hydrolysis rate on properties of nanosized TiO_2 synthesized via sol-gel hydrothermal. In: Advanced Materials Research. 2015. Trans Tech Publications.

[31] Su C, Tseng CM, Chen LF, You BH, Hsu BC, Chen SS. Sol-hydrothermal preparation and photocatalysis of titanium dioxide. Thin Solid Films. 2006;**498**(1–2):259–265. doi:10.1016/j.tsf.2005.07.123

[32] Su C, Hong BY, Tseng CM. Sol–gel preparation and photocatalysis of titanium dioxide. Catalysis Today. 2004;**96**(3):119–126. doi:10.1016/j.cattod.2004.06.132

[33] Yu JC, Zhang L, Yu J. Direct sonochemical preparation and characterization of highly active mesoporous TiO_2 with a bicrystalline framework. Chemistry of Materials. 2002;**14**(11):4647–4653. doi:10.1021/cm0203924

[34] Chen Z, Zhao G, Li H, Han G, Song B. Effects of water amount and pH on the crystal behavior of a TiO_2 nanocrystalline derived from a sol–gel process at a low temperature. Journal of the American Ceramic Society. 2009;**92**(5):1024–1029. doi:10.1111/j.1551-2916.2009.03047.x

[35] Bessekhouad Y, Robert D, Weber JV, Synthesis of photocatalytic TiO_2 nanoparticles: optimization of the preparation conditions. Journal of Photochemistry and Photobiology A: Chemistry. 2003;**157**(1):47–53. doi:10.1016/s1010-6030(03)00077-7

[36] Sergio Valencia, Marín JM, Restrepo G. Study of the bandgap of synthesized titanium dioxide nanoparticules using the sol-gel method and a hydrothermal treatment. The Open Materials Science Journal. 2010;**4**(1874-088X/10):9–14

[37] Oskam G, Nellore A, Penn RL, Searson PC. The growth kinetics of TiO_2 nanoparticles from titanium(IV) alkoxide at high water/titanium ratio. The Journal of Physical Chemistry B. 2003;**107**(8):1734–1738. doi:10.1021/jp021237f

[38] Venkatachalam V, Palanichamy M, Murugesan V. Sol–gel preparation and characterization of nanosizeTiO_2: Its photocatalytic performance. Materials Chemistry and Physics. 2007;**104**(2):554–559

[39] Yu JC, Yu J, Zhang L, Ho W. Enhancing effects of water content and ultrasonic irradiation on the photocatalytic activity of nano-sized TiO_2 powders. Journal of Photochemistry and Photobiology A. 2002;**148**(1–3):263–271. doi:10.1016/s1010-6030(02)00052-7

[40] Behnajady MA, Eskandarloo H, Modirshahla N, Shokri M. Investigation of the effect of sol–gel synthesis variables on structural and photocatalytic properties of TiO_2 nanoparticles. Desalination. 2011;**278**(1–3):10–17. doi:10.1016/j.desal.2011.04.019

[41] Kazuhiko M. Photocatalytic water splitting using semiconductor particles: History and recent developments. Journal of Photochemistry and Photobiology C: Photochemistry Reviews. 2011;**12**(4):237–268. doi:10.1016/j.jphotochemrev.2011.07.001

[42] Kudo A. Photocatalysis and solar hydrogen production. Pure and Applied Chemistry. 2007;**79**(11):1917–1927

[43] Subramanian V, Wolf EE, Kamat PV. Catalysis with TiO_2/gold nanocomposites. Effect of metal particle size on the fermi level equilibration. Journal of the American Chemical Society. 2004;**126**(15):4943–4950. doi:10.1021/ja0315199

[44] Leung DYC, Fu X, Wang C, Ni M, Leung MKH, Wang X, Fu X. Hydrogen production over titania-based photocatalysts. ChemSusChem. 2010;**3**(6):681-694. DOI: 10.1002/cssc.201000014

[45] Naseri N, Kim H, Choi W, Moshfegh AZ. Optimal Ag concentration for H_2 production via Ag:TiO_2 nanocomposite thin film photoanode. International Journal of Hydrogen Energy. 2012;**37**(4):3056-3065. http://dx.doi.org/10.1016/j.ijhydene.2011.11.041

[46] Lalitha K, Sadanandam G, Kumari VD, Subrahmanyam M, Sreedhar B, Hebalkar NY. Highly stabilized and finely dispersed Cu_2O/TiO_2: A promising visible sensitive photocatalyst for continuous production of hydrogen from glycerol:water mixtures. The Journal of Physical Chemistry C. 2010;**114**(50):22181–22189. doi:10.1021/jp107405u

[47] Malato S, Fernández-Ibáñez P, Maldonado MI, Blanco J, Gernjak W. Decontamination and disinfection of water by solar photocatalysis: Recent overview and trends. Catalysis Today. 2009;**147**(1):1–59. doi:10.1016/j.cattod.2009.06.018

[48] Ni M, Leung MKH, Leung DYC, Sumathy K. A review and recent developments in photocatalytic water-splitting using TiO_2 for hydrogen production. Renewable and Sustainable Energy Reviews. 2007;**11**(3):401–425. doi:10.1016/j.rser.2005.01.009

[49] Gombac V, Sordelli L, Montini T, Delgado JJ, Adamski A, Adami G, Cargnello M, Bernal S, Fornasiero P. CuOx–TiO_2 photocatalysts for H_2 production from ethanol and glycerol

solutions. The Journal of Physical Chemistry A. 2009;**114**(11):3916–3925. doi:10.1021/jp907242q

[50] Ghasemi S, Rahimnejad S, Setayesh SR, Rohani S, Gholami MR. Transition metal ions effect on the properties and photocatalytic activity of nanocrystalline TiO_2 prepared in an ionic liquid. Journal of Hazardous Materials. 2009;**172**(2–3):1573–1578. doi:10.1016/j.jhazmat.2009.08.029

[51] Sreethawong T, Suzuki Y, Yoshikawa S. Photocatalytic evolution of hydrogen over mesoporous supported NiO photocatalyst prepared by single-step sol–gel process with surfactant template. International Journal of Hydrogen Energy. 2005;**30**(10):1053–1062

[52] Singh AP, Kumari S, Shrivastav R, Dass S, Satsangi VR. Iron doped nanostructured TiO_2 for photoelectrochemical generation of hydrogen. International Journal of Hydrogen Energy. 2008;**33**(20):5363–5368. doi:10.1016/j.ijhydene.2008.07.041

[53] Kim A-Y, Kang M. Effect of Ag-Cu bimetallic components in a TiO_2 framework for high hydrogen production on methanol/water photo-splitting. International Journal of Photoenergy. 2012;**2012**(2012):1–9. doi:10.1155/2012/618642

[54] Sun T, Liu E, Fan J, Hu X, Wu F, Hou W, Yang Y, Kang L. High photocatalytic activity of hydrogen production from water over Fe doped and Ag deposited anatase TiO_2 catalyst synthesized by solvothermal method. Chemical Engineering Journal. 2013;**228**:896–906. doi:10.1016/j.cej.2013.04.065

IntechOpen